Raman Spectroscopic Study of Saturated Mixed-Chain Phosphatidylcholine Multilamellar Dispersions†

C. Huang,*,‡ J. T. Mason, and I. W. Levin*

ABSTRACT: The thermotropic behavior of a series of mixed-chain saturated phospholipids in fully hydrated multilamellar dispersions has been examined by vibrational Raman spectroscopy in both the C–C stretching (1000–1200-cm^{-1}) and the C–H stretching (2800–3100-cm^{-1}) mode regions. This lipid series represents phosphatidylcholines in which the *sn*-1 acyl chain is fixed in length with 18 carbon atoms, while the *sn*-2 acyl chain length is increased in steps of two methylene units from 10 to 18 carbon atoms. The transition temperatures of these mixed-chain phosphatidylcholines measured by Raman spectroscopic procedures are in good agreement with those determined by high-sensitivity differential scanning calorimetry. The total change in the Raman spectral intensity ratio $\Delta(I_{2935cm^{-1}}/I_{2884cm^{-1}})$ across the narrow gel ↔ liquid-crystalline phase transition temperature region is markedly different for the mixed-chain phospholipids in comparison to the symmetric chain systems. For the mixed-chain bilayer dispersions, the data conform to a smooth hyperbolic cosine curve and vary in the order C(18):C(10)PC > C(18):C(12)PC > C(18):C(14)PC < C(18):C(16)PC < C(18):C(18)PC with a minimum chain–chain order/disorder change observed for the C(18):C(14)PC multilamellar assemblies. The change in the spectral intensity ratio determined in the 1000–1200-cm^{-1} region is similar to that detected in the 2800–3100-cm^{-1} region; the smallest change in the spectral intensity ratio $\Delta(I_{1088cm^{-1}}/I_{1065cm^{-1}})$ across the phase transition region is again observed for the C(18):C(14)PC dispersions. These data, together with other structural information determined at common reduced temperatures for various gel state, mixed-chain phospholipid dispersions, lead to the conclusion that membrane lipids adopt two types of chain conformations in bilayer systems. In the first class, the lipid molecules in the two opposing monolayers pack independently, as typified by the C(18):C(18)PC and C(18):C(16)PC bilayers. In contrast, the hydrocarbon chains in the second type of lipid bilayers are assumed to effect an interdigitated packing arrangement which couples the two monolayers across the bilayer center. This second type of bilayer is represented by the C(18):C(10)PC, C(18):C(12)PC, and C(18):C(14)PC dispersions.

Lamellar phospholipids in excess water have been extensively studied as a model for understanding the structure and properties of the complex lipid matrices of biological membranes. Of the many characteristics associated with the bilayer lamellar structure of phospholipids, the endothermic gel ↔ liquid-crystalline phase transition is perhaps the property most extensively studied. It is now well documented that the behavior of the main phase transition depends on the acyl chain length, the degree of unsaturation of the phospholipid acyl chains, the head group of the phospholipid, the pH and ionic environment of the aqueous media, and the hydrostatic pressure (Quinn, 1981; McElhaney, 1982). Most of the reported physical studies on gel ↔ liquid-crystalline phase transitions, however, were limited to a specific class of synthetic symmetric phospholipids, since these systems could be obtained commercially with a reasonably high degree of purity. Recently, we have developed a method for synthesizing various species of mixed-chain phosphatidylcholines with ~98 mol % purity (Mason et al., 1981a). The gel ↔ liquid-crystalline phase transition behavior of dispersions of the mixed-chain phosphatidylcholines was studied by high-sensitivity, differential scanning calorimetry (Mason et al., 1981b). The thermal data suggested that when the number of methylene units in the *sn*-2 chain becomes fewer than those in *sn*-1 chain by four or more, as in the 1-stearoyl-2-lauroyl-*sn*-glycero-3-phosphocholine [C(18):C(12)PC][1] and C(18):C(10)PC dispersions, these highly asymmetric phosphatidylcholine molecules form interdigitated gel-state bilayers in such a manner that the shorter chain of one lipid in a leaflet packs end to end with the longer chain of another lipid in the opposing bilayer leaflet.

In the present paper, we report our Raman spectroscopic investigations of the mixed-chain phosphatidylcholine dispersions in excess water. We believe this to be the first time that vibrational Raman spectroscopy has been applied toward investigating the behavior of mixed-chain phospholipid bilayers. Specifically, we have examined the Raman spectral changes, as a function of temperature, in the hydrocarbon chain C–H and C–C stretching mode regions for a series of phosphatidylcholines in which the *sn*-1 acyl chain is fixed in length at 18 carbon atoms, while the *sn*-2 acyl chain length is increased in steps of two methylene units from 10 to 18 carbon atoms. Our results provide structural evidence which argues in favor of a model for acyl chains of highly asymmetric phosphatidylcholines being interdigitated in the gel-state bilayer. Moreover, for the five phosphatidylcholine bilayer systems studied, the spectroscopic parameter ΔI_R^{CH}, which represents the overall changes in the Raman peak height intensity ratios $I_{2935cm^{-1}}/I_{2884cm^{-1}}$ across the gel ↔ liquid-crystalline phase transition region, correlates linearly with ΔS, the transition

† From the Laboratory of Chemical Physics, National Institute of Arthritis, Diabetes, and Digestive and Kidney Diseases, National Institutes of Health, Bethesda, Maryland 20205 (C.H. and I.W.L.), and the Department of Biochemistry, University of Virginia School of Medicine, Charlottesville, Virginia 22908 (J.T.M.). *Received December 7, 1982; revised manuscript received March 4, 1983.* This investigation was supported in part by Research Grant GM-17452 from the National Institute of General Medical Sciences, U.S. Public Health Service.

‡ On sabbatical leave (1981–1982) from the Department of Biochemistry, University of Virginia School of Medicine, Charlottesville, VA 22908.

[1] Abbreviations: C(18):C(10)PC, 1-stearoyl-2-caproyl-*sn*-glycero-3-phosphocholine; C(18):C(12)PC, 1-stearoyl-2-lauroyl-*sn*-glycero-3-phosphocholine; C(18):C(14)PC, 1-stearoyl-2-myristoyl-*sn*-glycero-3-phosphocholine; C(18):C(16)PC, 1-stearoyl-2-palmitoyl-*sn*-glycero-3-phosphocholine; C(18):C(18)PC, L-α-distearoylphosphatidylcholine.

entropy determined previously by high-sensitivity differential scanning calorimetry.

Materials and Methods

High-purity (≥98 mol %) samples of C(18):C(16)PC, C(18):C(14)PC, C(18):C(12)PC, and C(18):C(10)PC were synthesized by phospholipase A_2 digestion of distearoylphosphatidylcholine, followed by reacylation of the 1-stearoyllysophosphatidylcholine with the appropriate fatty acid anhydride, using the catalyst 4-pyrrolidinopyridine (Mason et al., 1981a). The formation of positional isomers from acyl chain migration between the *sn*-1 and *sn*-2 chains of the glycerol backbone is less than 2% under the experimental conditions. C(18):C(18)PC was purchased from Avanti Biochemicals, Inc.

In general, 6–10 mg of lyophilized mixed-chain phosphatidylcholine was dispersed in an appropriate volume of 75 mM NaCl–7.5 mM phosphate buffer solution, pH 7.0, to form a sample with a lipid concentration of 33.3% (w/w) in a final solution of 50 mM NaCl–5 mM phosphate buffer. The coarse dispersion was incubated at a temperature 10–15 °C above the phase transition temperature and was vortexed several times for about 2–3 min at this elevated temperature. The dispersion was pipetted into a glass capillary (1.25-mm i.d.) and then spun in a bench-top clinical centrifuge at room temperature. After the capillary was sealed, the sample was allowed to anneal at 0 °C for a minimum for 3 days prior to use.

Raman spectra of the mixed-chain phosphatidylcholine dispersions in the vibrational C–H and C–C stretching regions were obtained with a Spex Ramalog 6 spectrometer equipped with holographic gratings and interfaced to a Nicolet NIC-1180 data acquisition system. The Raman instrumentation and the detailed procedures for determining the melting behavior of phospholipid dispersions have been described elsewhere (Lavialle & Levin, 1980; Huang et al., 1982). In general, Raman spectra were recorded at a scanning rate of 1 cm^{-1}/s with a laser excitation power of 200–220 mW from an argon ion source. Spectral frequencies are reported to ±2 cm^{-1}. All temperature profiles were recorded in an ascending temperature direction, and, at any given temperature, a thermal equilibration time of 12–15 min was allowed for the sample prior to Raman spectral collections. The temperature was monitored by a copper–constantan thermocouple inserted into the thermostatically controlled sample holder near the sample position. No temperature corrections were made for possible local heating of the sample from the relatively low incident laser power levels.

Results

Skeletal C–C Stretching Modes: 1000–1200-cm^{-1} Region. Figure 1 displays Raman spectra in the 1000–1200-cm^{-1} region for C(18):C(14)PC dispersions at five temperatures. At low gel phase temperatures, four primary C–C stretching mode features are observed at approximately 1065, 1088, 1106, and 1132 cm^{-1}. The assignments of these bands for symmetric diacylphosphatidylcholines have been discussed in the literature [see, for example, Lippert & Peticolas (1972) and Vogel & Jähnig (1981)]. The intense 1065- and 1132-cm^{-1} peaks are attributed to the out-of-phase and in-phase skeletal carbon–carbon (C–C) stretching modes for the all-trans states, respectively. The 1106-cm^{-1} peak also originates from a C–C skeletal motion in an all-trans state but for a phase difference between neighboring adjacent carbon oscillators other than 0 or π. The peak centered around 1088 cm^{-1} arises from C–C stretching modes for gauche conformers. It is evident from

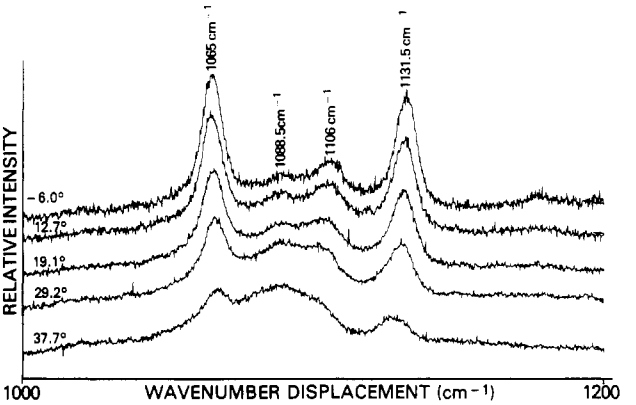

FIGURE 1: Raman spectra of the 1000–1200-cm^{-1} skeletal C–C stretching mode region for C(18):C(14)PC dispersions at temperatures spanning the gel and liquid-crystalline bilayer phases. Frequencies for only the −6 °C spectrum for the gel state are noted.

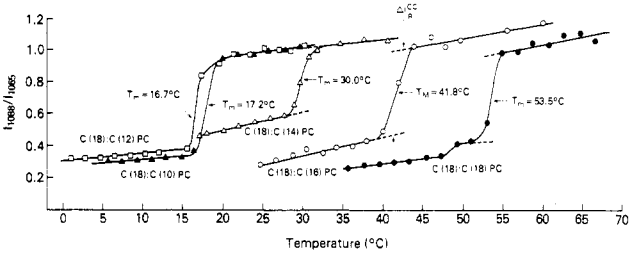

FIGURE 2: Temperature profiles for various mixed-chain stearoylphosphatidylcholine dispersions derived from the Raman spectral $I_{1088cm^{-1}(gauche)}/I_{1065cm^{-1}}$ peak height intensity ratios.

Figure 1 that with increasing temperature, the 1088-cm^{-1} feature increases in intensity, while the remaining three features decrease in intensity as gauche isomers are introduced into the all-trans chain. The most significant increase in the relative peak height intensity ratio $I_{1088cm^{-1}}/I_{1065cm^{-1}}$ occurs between 29.7 and 30.8 °C when C(18):C(14)PC undergoes the gel ↔ liquid-crystalline phase transition (Figure 2). The significance of the temperature-dependent changes in various band intensities and peak frequencies for phospholipid dispersions in the 1000–1200-cm^{-1} region has been discussed previously (Levin & Bush, 1981). We emphasize that the relative intensity ratio $I_{1088cm^{-1}}/I_{1065cm^{-1}}$ provides a sensitive spectral index for monitoring, as a function of temperature, the intramolecular order/disorder characteristics of the hydrocarbon region of lamellar phospholipids in excess water.

For various mixed-chain phosphatidylcholine dispersions, Figure 2 displays the temperature profiles derived from the Raman spectral index $I_{1088cm^{-1}}/I_{1065cm^{-1}}$. At a characteristic temperature, each lipid dispersion exhibits an abrupt, large increase in conformational disorder. It has been shown previously for symmetric diacylphosphatidylcholine dispersions that the sudden change in conformational disorder corresponds to the endothermic gel ↔ liquid-crystalline phase transition detected by calorimetry [for recent reviews, see Lord & Mendelsohn (1981) and Levin (1983)]. The temperature corresponding to the midpoint of this conformational order/disorder transition is taken as the transition temperature (T_m) of the mixed-chain phosphatidylcholine dispersions. The values of T_m are presented in Table I. In addition, the values of ΔI_R^{CC} for the different lipid dispersions are also presented in Table I. Here, ΔI_R^{CC} is the total change, estimated at T_m, in the Raman spectral index (for the C–C stretching region) across the order/disorder transition; it is determined from the extended linear portions of the upper and lower ends of the transition curve at T_m, as denoted in Figure 2.

Table I: Raman Spectroscopic and Thermal Data for Mixed-Chain Phosphatidylcholine Dispersions

n[a]	T_m^{CC}[b] (°C)	T_m^{CH}[c] (°C)	T_m^{calor}[d] (°C)	ΔS (eu/mol)[d]	$I_{1088cm^{-1}}/I_{1065cm^{-1}}$[e]	$I_{1088cm^{-1}}/I_{1130cm^{-1}}$[e]	ΔI_R^{CC}[f]	$I_{2935cm^{-1}}/I_{2884cm^{-1}}$[e]	ΔI_R^{CH}[g]
10	17.2	17.2	19.7, 20.2	34.5	0.31	0.46	0.59	0.39	0.38
12	16.7	16.8	18.5	26.4	0.34	0.46	0.54	0.38	0.31
14	30.0	29.1	29.9, 30.1	18.5	0.50	0.65	0.40	0.48	0.23
16	41.8	41.6	44.1	22.7	0.36	0.49	0.52	0.45	0.27
18	53.5	53.6	55.1	31.4	0.31	0.42	0.54	0.39	0.34

[a] Number of carbon atoms in C(18):C(n)PC. [b] T_m determined from temperature profiles constructed from spectral parameters derived from the C-C stretching region (1000-1200 cm^{-1}). [c] T_m determined from temperature profiles constructed from spectral parameters derived from the C-H stretching region (2800-3100 cm^{-1}). [d] Calorimetric values for T_m and ΔS (Mason et al., 1981b). [e] Peak height intensity ratios at a temperature 10 °C below T_m. [f] Change in Raman peak height intensity ratios ($I_{1088cm^{-1}}/I_{1065cm^{-1}}$) across the main phase transition at T_m. [g] Change in Raman peak height intensity ratios ($I_{2935cm^{-1}}/I_{2884cm^{-1}}$) across the main phase transition at T_m.

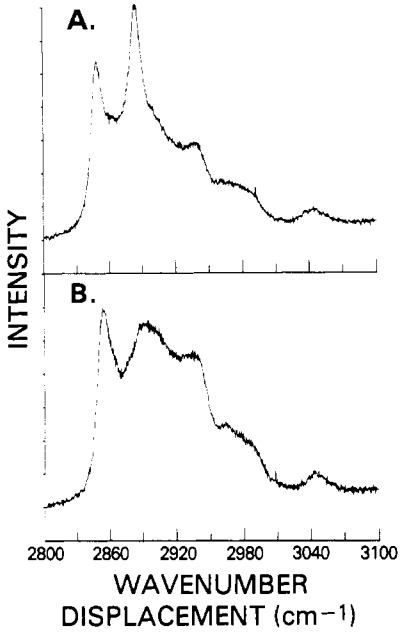

FIGURE 3: Raman spectra of C(18):C(10)PC dispersions: (A) the gel state at 20 °C; (B) the liquid-crystalline state at 42 °C.

C–H Stretching Modes: 2800–3100-cm^{-1} Region. In general, the C–H stretching mode region is used to monitor intermolecular chain–chain packing order/disorder alterations in membranes. The Raman vibrational transitions attributed to the methyl and methylene distortions in the C–H stretching mode interval (2800–3100 cm^{-1}) are generally about a factor of 3 more intense than features in the C–C stretching mode region (1000–1200 cm^{-1}). As shown in Figure 3A for the gel-state C(18):C(10)PC dispersions at 20 °C, the vibrationally congested 2800–3100-cm^{-1} spectral region consists of a number of vibrational transitions associated with the acyl chain moiety. The symmetric and asymmetric methylene C–H stretching modes appear as intense, partially overlapped features at 2849 and 2884 cm^{-1}, respectively. One Fermi resonance component of the symmetric C–H stretching mode for the chain-terminal methyl group occurs at 2935 cm^{-1}, while the chain-terminal methyl asymmetric C–H stretching modes appear around 2960 cm^{-1}. The broad features corresponding to the head-group choline symmetric and asymmetric methyl C–H stretching modes appear in the 2980- and 3042-cm^{-1} regions, respectively. A broad contour underlying the 2884-cm^{-1} band is assumed to arise from the Fermi resonance interaction between the symmetric methylene C–H stretching fundamental at 2850 cm^{-1} and the continuum of binary combinations of the methylene bending fundamentals of the extended hydrocarbon chains near 1450 cm^{-1} (Snyder et al., 1978; Snyder & Scherer, 1979). Above the gel ↔ liquid-crystalline phase transition temperature, the Fermi resonance interaction is diminished

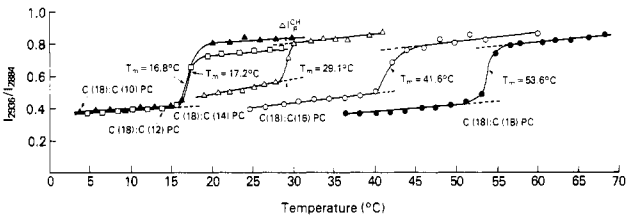

FIGURE 4: Temperature profiles for various mixed-chain stearoylphosphatidylcholine dispersions derived from the Raman spectral $I_{2935cm^{-1}}/I_{2884cm^{-1}}$ peak height intensity ratios.

as a result of vibrational decoupling caused by the conversion along the acyl chain of a significant number of C–C trans bonds to gauche isomers. Consequently, the intensity of the 2884-cm^{-1} band appears to decrease significantly, as seen in Figure 3B for the C(18):C(10)PC dispersion in the liquid-crystalline state at 42 °C. Further, an underlying manifold of infrared-active, Raman-inactive, methylene asymmetric stretching modes lies beneath the 2935-cm^{-1} feature for the all-trans acyl chain configuration. These modes, however, become Raman allowed, considering local chain symmetry, and contribute to the Raman C–H stretching mode region as the chain symmetry is broken when the bilayer undergoes chain melting (Bunow & Levin, 1977). It is seen from Figure 3A that the 2935-cm^{-1} feature is relatively weak in intensity when the lamellar phospholipids are in the gel state. In contrast, the 2935-cm^{-1} feature becomes relatively more intense in the liquid-crystalline state, as shown in Figure 3B, perhaps due, in part, to the effect of the change in physical state on the Fermi resonance interaction displayed by the methyl symmetric stretching modes (Hill & Levin, 1979). Because of the high sensitivity of the 2884- and 2935-cm^{-1} features toward the alterations in chain packing characteristics, the Raman peak height intensity ratio of these two features, $I_{2935cm^{-1}}/I_{2884cm^{-1}}$, has been used as a convenient monitor of the interchain order/disorder processes of the lipid components in bilayers (Yellin & Levin, 1977a,b).

Figure 4 shows the temperature dependence of the Raman peak height intensity ratio $I_{2935cm^{-1}}/I_{2884cm^{-1}}$ for the various mixed-chain phosphatidylcholine dispersions. Similar to the temperature profiles shown in Figure 2, an abrupt increase in chain–chain disorder is observed within a very narrow temperature range for each of the lipid dispersions. The transition temperatures, T_m, determined from the temperatures corresponding to the midpoints of the temperature profiles, are presented in Table I. It is seen that the values of T_m determined in the 2800–3100-cm^{-1} region agree quite well with those determined from the 1000–1200-cm^{-1} region spectral parameters.

The spectroscopic parameters, ΔI_R^{CH}, which represent the total changes in amplitude at T_m for the Raman intensity ratios obtained from the C–H stretching mode region, are determined

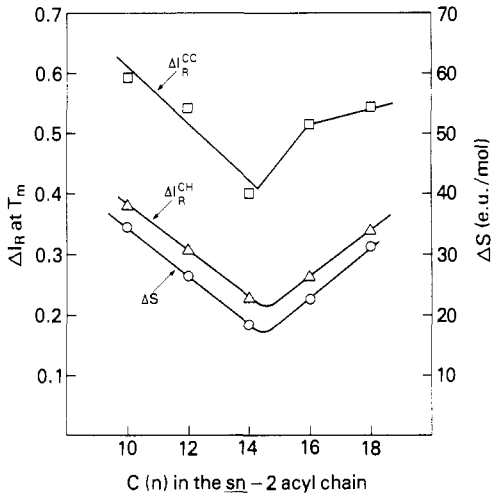

FIGURE 5: Behavior of ΔI_R^{CH}, ΔI_R^{CC}, and ΔS as a function of the length of the *sn*-2 acyl chain. (See text for definitions of ΔI_R^{CH} and ΔI_R^{CC}.)

from the temperature profiles in Figure 4 and are tabulated in Table I. Figure 5 displays the values of ΔI_R^{CC} and ΔI_R^{CH} as a function of the *sn*-2 chain length. The transition entropy (ΔS) is also included in Figure 5. We note that for the five phosphatidylcholine–water systems examined, the spectroscopic parameters ΔI_R^{CH} for the asymmetric lipids are also linearly correlated to ΔS. The derived expression yields $\Delta I_R^{CH} = (9.04 \times 10^{-3})\Delta S + 0.065$, with a correlation coefficient of 0.995.

Discussion

The thermotropic behavior of mixed-chain saturated phosphatidylcholines in multilamellar dispersions has been examined principally by high-sensitivity, differential scanning calorimetry, although the early studies employed mixed-chain phospholipids which are frequently isomerically impure and exhibited limited chain length differences (Keough & Davis, 1979; Chen & Sturtevant, 1981; Stümpel et al., 1981). In a recent investigation (Mason et al., 1981b), the previous studies were extended by systematically varying the chain lengths of saturated mixed-chain phosphatidylcholines to include differences of two, four, six, and eight methylene units. This study led to a model which suggested that the thermotropic behavior of the mixed-chain phosphatidylcholines results from progressively increased interdigitation of the acyl chains across the gel-state bilayer for chain length differences beyond a minimum value (Mason et al., 1981b).

In this paper, the thermotropic behavior of multilamellar dispersions of highly purified, mixed-chain phosphatidylcholines has been investigated by Raman spectroscopy. Although the transition temperatures of these lipid dispersions as determined by Raman spectroscopy (Table I) are in reasonably good agreement with the corresponding values obtained by differential scanning calorimetry, the values of T_m measured by the Raman spectroscopic technique are, in general, lower by ~0.5–2.0 °C. This difference may, in part, arise from local heating effects due to the incident laser radiation.

In the gel state, the relative gauche/trans population along the acyl chain in the various mixed-chain phosphatidylcholine dispersions may be compared at a common temperature relative to T_m. It can be seen from Figure 2 and the $I_{1088cm^{-1}}/I_{1065cm^{-1}}$ ratios given in Table I for temperatures 10 °C below T_m that the relative gauche/trans population is the greatest for the multilayers formed from the C(18):C(14)PC species. The degree of intrachain disorder for the series of phospholipids presented in Figure 2 has the following sequence: C(18):C(14)PC > C(18):C(16)PC > C(18):C(12)PC > C(18):C(10)PC = C(18):C(18)PC. The values for the intensity ratios, which are reported to ±5%, appear in Table I, column 6.

The relative strengths of the intermolecular chain–chain interactions for the various mixed-chain phosphatidylcholines can also be estimated from Figure 4. Again, at a temperature 10 °C below T_m, the value of $I_{2935cm^{-1}}/I_{2884cm^{-1}}$ listed in Table I for the C(18):C(14)PC system in the gel-state bilayer is the largest for the series examined, indicating that the intermolecular chain–chain interactions in the hydrocarbon chain region of the C(18):C(14)PC bilayers are the weakest (Table I, column 9). The relative degree of intermolecular disorder for the series of phospholipids varies as follows: C(18):C(14)PC > C(18):C(16)PC > C(18):C(10)PC = C(18):C(18)PC ≅ C(18):C(12)PC; that is, similar to the order observed above for the $I_{1088cm^{-1}}/I_{1065cm^{-1}}$ ratios (Figure 2 and Table I).

The observation that in the gel state the disordering characteristics follow the general patterns described above is explicable from a model in which the terminal segment of the longer *sn*-1 chain perturbs both the intrachain conformational statistics as well as the interactions between chains (Mason et al., 1981b). That is, as the two chains become inequivalent in length, the terminal segment of the longer *sn*-1 chain is expected to undergo trans ↔ gauche isomerization to fill the void space under the contiguous, shorter *sn*-2 chain near the bilayer center. However, when the *sn*-1 chain is longer than the *sn*-2 chain by four or more methylene units in the mixed-chain phosphatidylcholine molecules, the mixed-chain lipids in the gel-state bilayer are proposed to adopt a configuration involving an interdigitated packing arrangement across the center of the bilayer (Mason et al., 1981b). An interdigitated configuration compensates for the chain inequivalence, while simultaneously increasing the stability of the bilayer state. Thus, for the series of mixed-chain phospholipids C(18):C(18)PC, C(18):C(16)PC, and C(18):C(14)PC, we propose that the bilayer gel state transforms from one where the two leaflets are discrete [C(18):C(18)PC and C(18):C(16)PC] to one where the two leaflets are just beginning to interdigitate [C(18):C(14)PC]. Further, the gel state of the C(18):C(14)PC bilayer is proposed to be strongly disordered toward the methyl ends as a consequence of the close proximity of the sterically large terminal methyl groups forming the slightly interdigitated bilayer (Mason et al., 1981b).

For the series C(18):C(14)PC, C(18):C(12)PC, and C(18):C(10)PC, an interdigitated bilayer is proposed for the gel state of these mixed-chain phosphatidylcholines. As the chain length inequivalence is increased, the terminal methyl groups move from the center of the hydrocarbon core of the bilayer. This situation increases the conformational stability of the gel state, since the bulky methyl groups tend to be less disruptive as they approach the structurally restrictive interface region (Mason et al., 1981b). On the basis of these arguments, we expect the intra- and interchain disorder in the bilayer gel state to follow the sequence C(18):C(14)PC > C(18):C(12)PC > C(18):C(10)PC. The Raman data, in general, indicate this trend and support the view that C(18):C(14)PC multilayers are the most disordered of the three species.

It is well established for C(18):C(18)PC bilayers in the gel state that the phospholipid acyl chains are packed in a nearly all-trans configuration (one to three gauche conformers per chain) and are oriented parallel to one another in order to maximize van der Waals contacts between chains (Gaber & Peticolas, 1977; Yellin & Levin, 1977a,b; Huang et al., 1982; Tardieu et al., 1973). From Figures 2 and 4, we note that at

a common reduced temperature in the gel state the degree of intra- and interchain disorder for the C(18):C(10)PC bilayer is equal to that for the symmetric chain C(18):C(18)PC. These observations argue persuasively for a gel-state bilayer conformation for C(18):C(10)PC dispersions in which the acyl chains, extended in an approximately all-trans configuration, are interdigitated in order to maximize interchain contacts. If the gel-state bilayer for the C(18):C(10)PC species is not interdigitated, one would then expect relatively large gauche/trans ratios, since the inequivalent ends of the longer *sn*-1 acyl chains would assume a high degree of rotomeric disorder in order both to fill the void volume at the terminus of the *sn*-2 chain and to increase van der Waals contacts between the chains of the separate, uncoupled bilayer leaflets. Although the temperature profiles in Figure 2 were constructed from the peak height intensity ratios $I_{1088cm^{-1}(gauche)}/I_{1065cm^{-1}}$, we also list the intensity ratios $I_{1088cm^{-1}(gauche)}/I_{1130cm^{-1}}$ in Table I for the mixed-chain phospholipids. In this comparison, $I_{1130cm^{-1}}$ is chosen as it is particularly sensitive to the trans segments of the acyl chains near the methyl termini [see, for example, Yellin & Levin (1977b)]. From the use of this index for monitoring acyl chain disorder, we again note that the C(18):C(14)PC bilayer exhibits the greatest gauche bond population, while the C(18):C(10)PC species is only slightly more disordered than the C(18):C(18)PC dispersions. Thus, the phospholipid species possessing the greatest degrees of chain inequivalence do not exhibit the increase of gauche conformers that would be expected for uncoupled bilayer leaflets.

In order to demonstrate more vividly the increase in packing order, which we suggest occurs for the interdigitated C(18):C(10)PC and C(18):C(12)PC species, we view in Figure 6 the series of spectra for the C–H stretching mode region recorded for the gel-state bilayers of the mixed-chain species at ~10 °C below T_m. Since the C–H stretching mode region of the bilayer system primarily reflects interchain interactions within the hydrophobic interior, we focus our attention upon the relative intensities of the methylene symmetric and asymmetric C–H stretching modes at approximately 2849 and 2884 cm^{-1}, respectively. The relative intensities and line widths of these modes reflect specific subcell crystal structures (Mushayakarara & Levin, 1982; Snyder et al., 1978). For the uncoupled C(18):C(18)PC bilayer system, the peak height intensity ratio $I_{2849cm^{-1}}/I_{2884cm^{-1}}$ is 0.84, a value close to 0.81 for C(16):C(16)PC dispersions. The ratio increases for the C(18):C(16)PC and C(18):C(14)PC bilayers to 0.92 and 0.97, respectively. Essentially, the broad background, which arises from the Fermi resonance couplings of the continuum of methylene deformation binary overtone combinations with the 2849-cm^{-1} fundamental and upon which the 2884-cm^{-1} feature sits, decreases due to lessened Fermi resonance interactions (Snyder et al., 1978). That is, as the acyl chain matrix becomes intra- and intermolecularly disordered, the depression of the Fermi resonance background derived from all-trans chain segments leads to a spectrum for which the two methylene stretching mode intensities tend to equalize. As the mixed-chain bilayer series continues to the C(18):C(12)PC and C(18):C(10)PC species, the ratios diverge to 0.74 and 0.79, respectively, indicating an increase in the Fermi resonance background beneath the 2884-cm^{-1} feature as a consequence of an increasing population of all-trans segments. For this to occur, the chains must interdigitate across the bilayer center.

Figure 5 presents the intermolecular order/disorder changes of the acyl chains across the gel ↔ liquid-crystalline phase

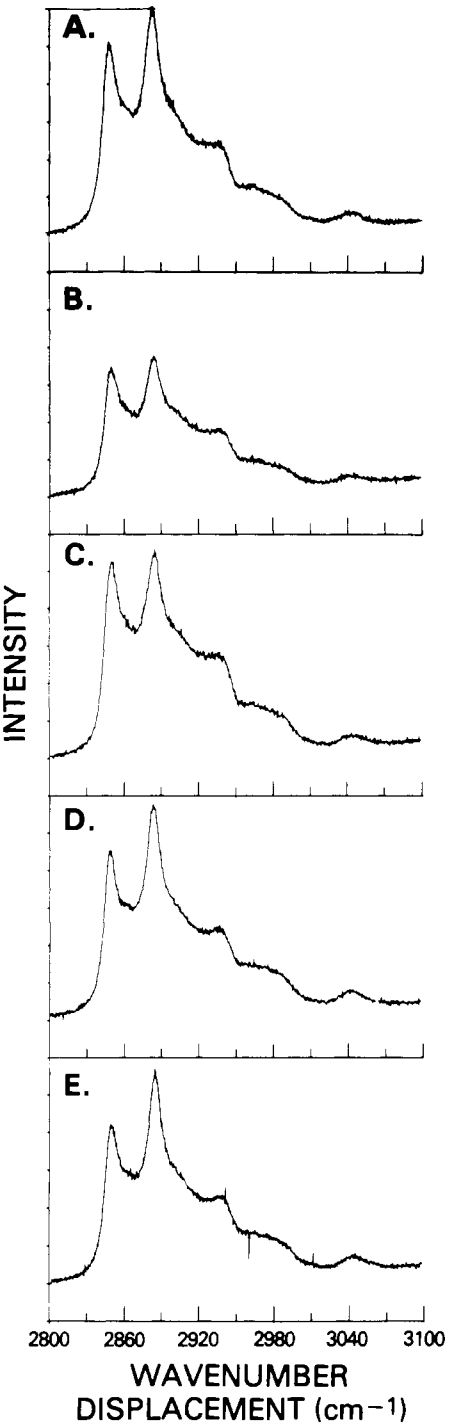

FIGURE 6: Comparison of the Raman spectra in the C–H stretching mode regions of various stearoylphosphatidylcholine dispersions recorded at ~10 °C below their respective T_m values. (A) C(18):C(18)PC; (B) C(18):C(16)PC; (C) C(18):C(14)PC; (D) C(18):C(10)PC; (E) C(18):C(12)PC.

transition region estimated at T_m for various mixed-chain phosphatidylcholine dispersions as a function of the *sn*-2 chain length. The values for ΔI_R^{CH} obtained in the C–H stretching region (2800–3100 cm^{-1}) appear to fall on a smooth curve for a hyperbolic cosine with a miminum observed for the C(18):C(14)PC multilamellar bilayers. This curve runs parallel to a plot derived from the transition entropy (ΔS) of the corresponding lipid dispersions determined by high-sensitivity, differential scanning calorimetry (Figure 5). This similarity is expected, since the transition entropy ΔS is a measure of the total entropy change (in terms of alterations within the hydrophobic and head-group regions) of the phospholipid–

water system associated with the gel ↔ liquid-crystalline phase transition at T_m. In this regard, a linear relationship between ΔI_R^{CH} and ΔS has been established for bilayers composed of saturated symmetric chain phosphatidylcholines with various chain lengths (Huang & Levin, 1982; Huang et al., 1982).

In Figure 5, ΔI_R^{CC}, the intramolecular order/disorder change across the gel ↔ liquid-crystalline phase transition region derived from C–C stretching mode region parameters, is also plotted as a function of the acyl chain length at the *sn*-2 position for a fixed *sn*-1 chain length of 18 carbon atoms. In comparison to the plot of ΔI_R^{CH} or ΔS against the *sn*-2 chain length, the deviation of ΔI_R^{CC} for the C(18):C(16)PC dispersion may be due to the difficulty in estimating the true base line for the main transition curve at the onset of the gel ↔ liquid-crystalline phase transition. Despite this uncertainty, the general order of C(18):C(10)PC > C(18):C(12)PC > C(18):C(14)PC < C(18):C(16)PC < C(18):C(18)PC observed for the intermolecular parameter ΔI_R^{CH} also holds for ΔI_R^{CC}.

In summary, we propose that the lipid bilayer adopts two types of chain packing configurations. In the first type, the lipid molecules within the two opposing leaflets of the bilayer pack independently; this bilayer is exemplified by C(18):C(18)PC and C(18):C(16)PC dispersions. Within this bilayer class, the longer the acyl chains and/or the smaller the chain inequivalence, the more stable the bilayer becomes in the gel state. The second type of bilayer packing occurs for lipid molecules whose acyl chains are interdigitated, as represented by the C(18):C(14)PC, C(18):C(12)PC, and C(18):C(10)PC assemblies. For this bilayer class, the greater the inequivalence between the two acyl chain lengths, the more stable is the gel-state bilayer dispersion. Although this model was originally suggested by differential scanning calorimetry (Mason et al., 1981b), the Raman data discussed here provide direct structural evidence for further substantiating an interpretation involving chain interdigitation to couple the bilayer leaflets. It is interesting to note that many natural membrane lipids, such as glycosphingolipids, sphingomyelin, cerebrosides, and sulfatides, are characterized by a large asymmetry in the length of their hydrocarbon chain moieties. These lipids, in particular, may display packing arrangements similar to the interdigitated class of bilayers addressed in this study, although most natural phospholipids would be expected to form dispersions analogous to the first type of noninterdigitated, or conformationally uncoupled bilayer leaflets.

Registry No. C(18):C(10)PC, 78119-50-3; C(18):C(12)PC, 7276-39-3; C(18):C(14)PC, 20664-02-2; C(18):C(16)PC, 59403-53-1; C(18):C(18)PC, 816-94-4.

References

Bunow, M., & Levin, I. W. (1977) *Biochim. Biophys. Acta 487*, 388–394.

Chen, S. C., & Sturtevant, J. M. (1981) *Biochemistry 20*, 713–718.

Gaber, B. P., & Peticolas, W. L. (1977) *Biochim. Biophys. Acta 465*, 260–274.

Hill, I. R., & Levin, I. W. (1979) *J. Chem. Phys. 70*, 842–851.

Huang, C., & Levin, I. W. (1982) in *Raman Spectroscopy: Linear and Nonlinear* (Lascombe, J., & Huong, P. V., Eds.) pp 759–760, Wiley, New York.

Huang, C., Lapides, J. R., & Levin, I. W. (1982) *J. Am. Chem. Soc. 104*, 5926–5930.

Keough, K. M. W., & Davis, P. J. (1979) *Biochemistry 18*, 1453–1459.

Lavialle, F., & Levin, I. W. (1980) *Biochemistry 19*, 6044–6050.

Levin, I. W. (1983) in *Advances in Infrared and Raman Spectroscopy* (Clark, R. J. H., & Hester, R. E., Eds.) Vol. II, Heyden, London (in press).

Levin, I. W., & Bush, S. F. (1981) *Biochim. Biophys. Acta 640*, 760–766.

Lippert, J. L., & Peticolas, W. L. (1972) *Biochim. Biophys. Acta 282*, 8–17.

Lord, R. C., & Mendelsohn, R. (1981) in *Membrane Spectroscopy* (Grell, E., Ed.) pp 377–426, Springer-Verlag, New York.

Mason, J. T., Broccoli, A. V., & Huang, C. (1981a) *Anal. Biochem. 113*, 96–101.

Mason, J. T., Huang, C., & Biltonen, R. L. (1981b) *Biochemistry 20*, 6086–6092.

McElhaney, R. N. (1982) *Chem. Phys. Lipids 30*, 229–259.

Mushayakarara, E., & Levin, I. W. (1982) *Biochim. Biophys. Acta 686*, 153–159.

Quinn, P. J. (1981) *Prog. Biophys. Mol. Biol. 38*, 1–104.

Snyder, R. G., & Scherer, J. R. (1979) *J. Chem. Phys. 71*, 3221–3228.

Snyder, R. G., Hsu, S. L., & Krimm, S. (1978) *Spectrochim. Acta, Part A 34A*, 395–406.

Stümpel, J., Nichsch, A., & Eibl, H. (1981) *Biochemistry 20*, 662–665.

Tardieu, A., Luzzati, V., & Reman, F. C. (1973) *J. Mol. Biol. 75*, 711.

Vogel, H., & Jähnig, F. (1981) *Chem. Phys. Lipids 29*, 83–101.

Yellin, N., & Levin, I. W. (1977a) *Biochemistry 16*, 642–647.

Yellin, N., & Levin, I. W. (1977b) *Biochim. Biophys. Acta 489*, 177–190.